Discovery of Further Pyrrolidine *trans*-Lactams as Inhibitors of Human Neutrophil Elastase (HNE) with Potential as Development Candidates and the Crystal Structure of HNE Complexed with an Inhibitor (GW475151)

Simon J. F. Macdonald,*,† Michael D. Dowle,*,† Lee A. Harrison,† Geoffrey D. E. Clarke,† Graham G. A. Inglis,† Martin R. Johnson,† Pritom Shah,† Robin A. Smith,‡ Augustin Amour,§ Gill Fleetwood,|| Davina C. Humphreys,‡ Christopher R. Molloy,‡ Mary Dixon,⊥ Rosalind E. Godward,⊥ Alan J. Wonacott,# Onkar M. P. Singh,# Simon T. Hodgson,† and George W. Hardy†

Medicinal Chemistry 1, In Vitro Pharmacology, Systems Research, Respiratory Systems, Stevenage CEDD DMPK, and Computational and Structural Sciences, GlaxoSmithKline Medicines Research Centre, Gunnels Wood Road, Stevenage SG1 2NY, United Kingdom

Received March 18, 2002

Described herein is a modern approach to the rapid preparation and evaluation of compounds as potential back-up drug candidates. GW311616A, **1**, a derivative of pyrrolidine *trans*-lactams, has previously been described as a potent, orally active inhibitor of human neutrophil elastase (HNE) for the treatment of respiratory disease. These properties made it a suitable candidate for development. Described here is the discovery of three further derivatives of pyrrolidine *trans*-lactams, which fulfill the criteria required for back-up candidates **28**, **29**, and **32**. These include increased activity in inhibiting HNE in human whole blood (HWB) and comparable pharmacokinetic properties, in particular clearance, in two species. To provide a rapid assessment of clearance, cassette dosing in dog was used. Modern array techniques, including the synthesis of mixtures, were used to synthesize compounds rapidly. Having selected three potential compounds as back-up candidates, they were prepared as single enantiomers and profiled in in vitro and in vivo assays and evaluated pharmacokinetically in rat and dog. These compounds are highly potent and selective HNE inhibitors, with a prolonged pharmacodynamic action. Pharmacokinetically, these compounds are comparable with **1** while they are more potent in HWB. Compound **28**, however, has a higher clearance. One of these compounds, **32**, was cocrystallized with HNE, and features of this structure are described and compared with the cocrystal structure of **1** in porcine pancreatic elastase.

Introduction

1. Background. A considerable body of work now describes inhibitors of human neutrophil elastase (HNE), a serine protease from the trypsin class, for the treatment of respiratory diseases such as chronic bronchitis, cystic fibrosis, and emphysema.[1] We have introduced pyrrolidine *trans*-lactams as inhibitors of HNE[2] and described some of their properties. In particular, we have described their intracellular mechanism and the medicinal chemistry program[3] that led to the discovery[4] of a drug candidate GW311616A **1** suitable for development.[5] The final phase of our program was to generate potential back-up development compounds in case **1** failed in the drug development phase. We describe here the goals for the back-up compounds and the medicinal chemistry strategy and its application using a library, pools, and array techniques. We report our development and use of cassette dosing in dog for the rapid evaluation of clearance. A summary of the biological data of the three potential back-up compounds and the crystal structure of one of these compounds in HNE is described. We particularly highlight the value of the cassette approach and the judicial use of modern medicinal chemistry techniques in aiding the rapid discovery of these back-up compounds. We also highlight the HNE crystal structure, one of very few published.

Although GW311616A was a suitable compound for development, it did contain features that were regarded as potential liabilities. From a structural viewpoint, we were keen to remove the acrylamide functionality since it was perceived as a potential toxicological risk because it is a Michael acceptor. There were also concerns over the long-term photostability of the double bond.[6] Considering the biological profile of **1**, the only available measure of its potential efficacy in humans is its potency, ex vivo in human whole blood (HWB) (0.67 μM). This is less potent than the Merck compound[7] L-694,458 (0.45 μM). We also noted that despite the excellent bioavailability of GW311616A in rat (60%) and dog (100%), its clearance in rat (79 mL/min/kg) and dog (28 mL/min/kg) approximated to liver blood flow (about 66 and 38 mL/min/kg, respectively).

These concerns directed our goals for the back-up compounds. Thus, our first two goals were to improve potency in HWB and maintain, if not reduce, the clearance in rat and dog. To address these goals, we could replace the piperidinocrotyl side chain and/or the

* To whom correspondence should be addressed. Fax: +44 1438 76 36 15. E-mail: sjfm5947@gsk.com and mdd3463@gsk.com.
† Medicinal Chemistry 1.
‡ In Vitro Pharmacology.
§ Systems Research.
|| Respiratory Systems.
⊥ Stevenage CEDD DMPK.
Computational and Structural Sciences.

10.1021/jm020881f CCC: $22.00
Published on Web 08/03/2002

pyrrolidine *trans*-lactam. We knew from previous structure−activity relationships (SAR) that most of the enzyme inhibitory activity of **1** is derived from the highly optimized *trans*-lactam core and that replacing this feature would be difficult and time-consuming. We therefore decided to replace the piperidinocrotyl side chain and keep the *trans*-lactam core intact. We were conscious, however, that the *trans*-lactam core might define threshold levels of potency in HWB and clearance rate whatever side chain was appended. To minimize this risk, we rapidly explored a wide range of piperidinocrotyl side chain replacements by using the latest medicinal chemistry technologies (libraries, arrays, and cassette dosing).

There were beneficial implications of this strategy. Initially, the back-up compounds would provide structural novelty and thereby further patent protection. The structural variety would also spread the risk in case of toxicity (assuming the toxicity is associated with the side chain). Second, we felt this synthetic program would be relatively straightforward. Third, if we were successful in improving potency in HWB, then this could reduce the cost of the medicine. A final major benefit was that if a back-up compound was required, then the *trans*-lactam core intermediate available from the multikilogram development synthesis of **1** could serve as a versatile intermediate to provide large quantities of the back-up compound quickly. This would minimize the amount of new synthetic development work required and reduce lead times−substantial benefits.

2. Setting Up the Screens and Cascade. We were keen to measure HWB potency and clearance early in the screening cascade in order to address our goals. We anticipated that screening against HWB[3] would be relatively straightforward for the numbers of compounds we would make from libraries and arrays. However, evaluating clearance using traditional pharmacokinetic assays has only a relatively low throughput. In general, the stability of the compounds to in vitro hepatic microsomes[3] precluded the use of the usual in vitro metabolic screens as predictors of plasma clearance. A rapid in vivo assessment of clearance was therefore required. The cassette dosing approach[8] potentially offered the high throughput required to rapidly identify analogues with similar/superior pharmacokinetics to **1**.

We therefore defined our screening cascade with narrowing filters as first in vitro assessment of inhibition potency against HNE and HWB followed by in vivo clearance in the dog using cassette dosing. The most promising compounds were then evaluated in in vivo assays, and full pharmacokinetic profiles were obtained.

3. Cassette Dosing Validation. Prior to its inclusion in the screening cascade, the cassette dosing technique was validated to ensure the absence of drug−drug interactions, which, on occasion, can undermine the predictive value of the estimated clearance rates. Five analogues, whose plasma clearance had previously been established in the dog, were coadministered together with three new pyrrolidine *trans*-lactams. A 1.6 mg/kg dose made up from 0.2 mg/kg of each of the eight compounds, was administered intravenously to a male beagle dog. (This dose level was selected to minimize interaction potential while ensuring that detectable plasma concentrations would be achieved.)

The results obtained (Figure 1) clearly show that the estimates of clearance, half-life, and volume generated using the cassette approach were in excellent agreement with those generated from definitive pharmacokinetic studies in which each compound was administered alone. This experiment validated the use of this approach as a high throughput means of assessing clearance of potential back-up compounds.

4. Cassette Protocol Design. The data generated from the validation study was used to optimize the experimental design and maximize compound throughput. Analysis of the data revealed a good inverse correlation between the plasma concentration measured 1 h after administration of the cassette dose and the plasma clearance ($r^2 = 0.835$). This correlation was underpinned by the similarity in volume of distribution of all of the analogues studied (3 L/kg). Given these findings and the relatively limited range in the physicochemical properties expected for the potential back-ups, the plasma concentration at 1 h was used as a measure of clearance. To correct for variability in the system, to ensure the integrity of the data generated, from each cassette, and to enable results to be easily compared with the project's lead, the racemate of **1**, compound **2**, was included in each cassette as an internal standard.

5. Medicinal Chemistry Strategy. The medicinal chemistry strategy was based principally upon the SAR learned from the discovery of **1**.[3,4] Modification of the piperidinocrotonyl side chain allows tuning of the pharmacodynamics and kinetics. The carbonyl is required for potency against HNE, the unsaturation gives a log unit increase in activity in vivo over the saturated analogue, and the amine, as its salt, provides solubility. We therefore decided (Figure 2) to explore surrogates

Scheme 1[a]

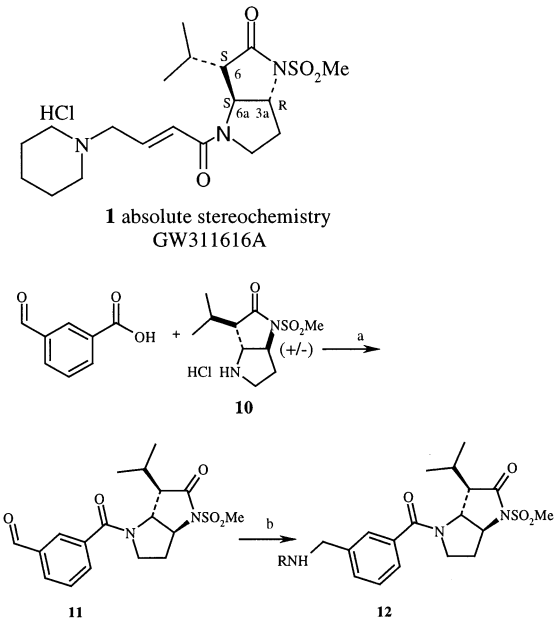

[a] All structures racemic. Reagents: (a) $Me_2N(CH_2)_3NCNEt\cdot HCl$ (EDC) (2 equiv), 1-hydroxybenzotriazole (HOBT) (2 equiv), **10**, MeCN, room temperature, 18 h, 39%. (b) Secondary amine (1.5 equiv), MeOH:CH_2Cl_2 (1:1) for 3 h and then BH_4^- on Amberlite IRA-400 (2.5 mmol/g) (approx 2 equiv), room temperature, 24 h and then polymer-bound benzaldehyde resin (0.27 mmol/g) (approx 1 equiv), 24 h.

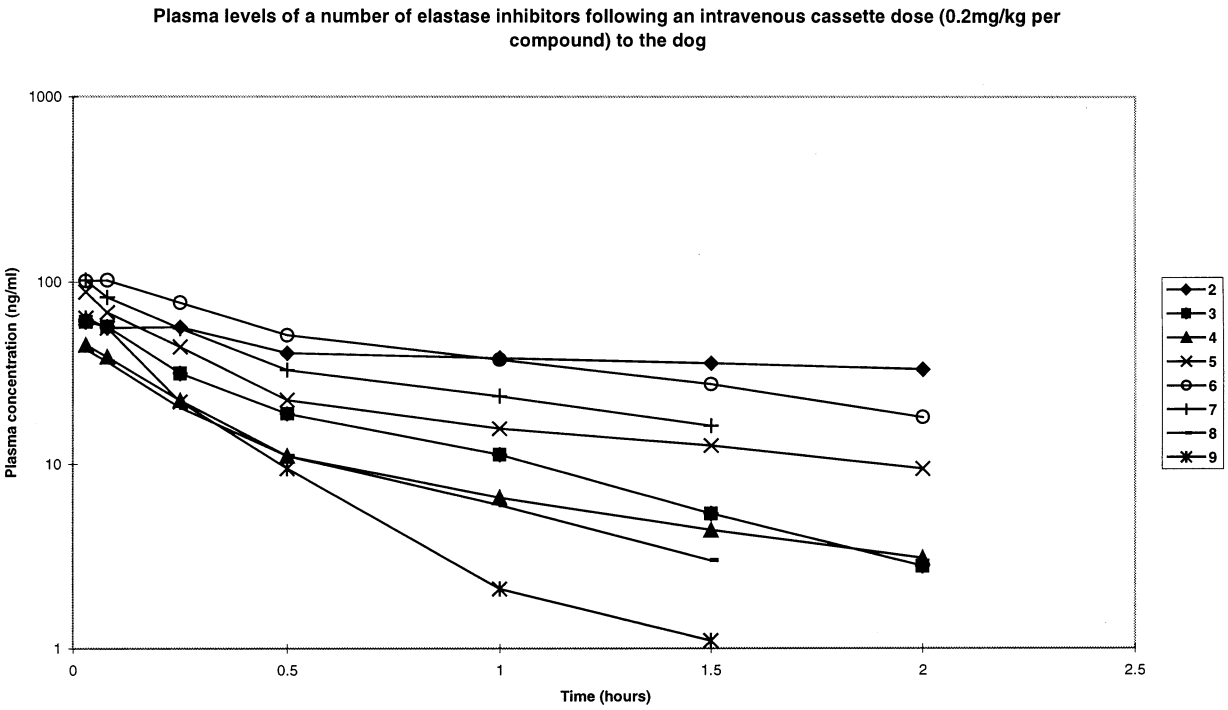

Parameter	Clp (mL/min/kg)		t1/2 (h)		Varea L/kg)	
	Cassette	Discrete	Cassette	Discrete	Cassette	Discrete
2	20	19	2	1.8	3.3	2.7
3	97	94	0.5	0.5	4.3	3.8
4	134	197	0.7	0.2	7.6	3.5
5	53	nd	1	nd	4.8	nd
6	28	40	1	0.9	2.5	2.9
7	46	nd	0.7	nd	2.9	nd
8	161	220	0.5	0.2	6.6	3.8
9	176	nd	0.3	nd	4.4	nd

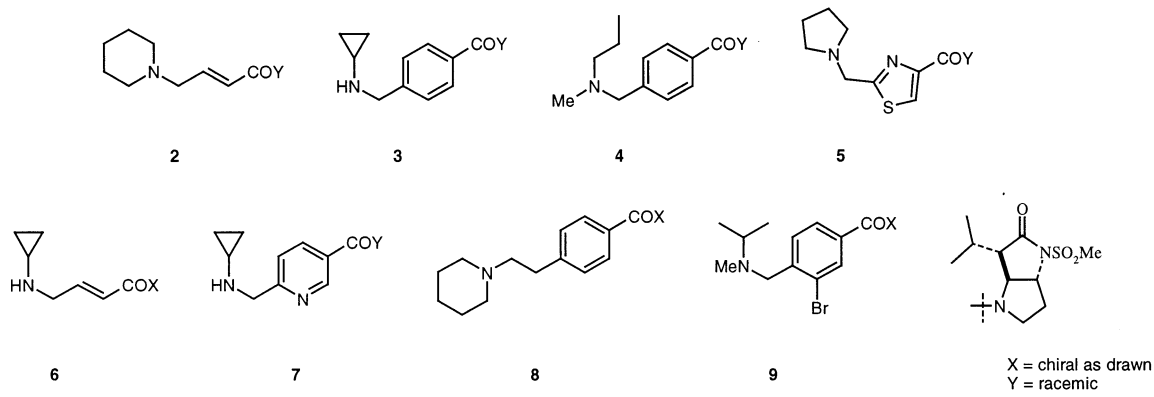

Figure 1. Details of the cassette validation experiment.

for the double bond, which would provide either π character and/or rigidity. We also selected diverse sets of amines based upon analyses of size (CMR), basicity (pK_a), and lipophilicity (clog*P*). Finally, we decided in the first instance to prepare racemates until potential back-up candidates had been identified. At the time, enantiomerically pure material was in short supply. This also safeguarded against the risk that the absolute stereochemistry of the enantiomer with the superior biological profile switched from that observed for **1**.[9]

6. 2° and 3° Benzylamines—Preparation and SAR. 6.1. Preparation. An array of 18 secondary amines (selected to represent diverse lipophilicity and molecular weight) was prepared using supported re-

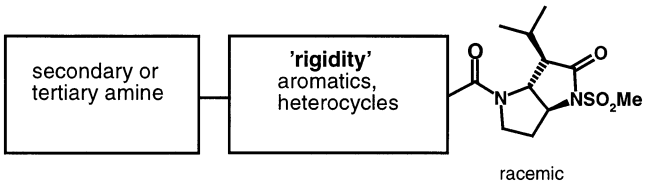

Figure 2. Cartoon summarizing the medicinal chemistry strategy.

Scheme 2[a]

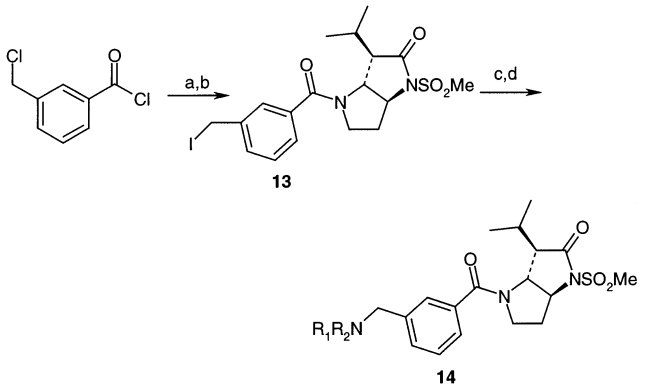

[a] All structures racemic. Reagents: (a) Compound **10** (0.77 equiv), $NaHCO_3$ (4 equiv), CH_2Cl_2, room temperature, 18 h, 42%. (b) NaI (3 equiv), Me_2CO, room temperature, 18 h, 97%. (c) R_1R_2NH (0.83 equiv), Amberlyst A-21 (excess), MeCN, room temperature, 2 h. (d) SCX bond elut purification.

agents (Scheme 1). The aldehyde **11** was prepared from 3-formylbenzoic acid and **10**. It was then treated with the primary amine for 3 h in 1:1 methanol:dichloromethane to preform the intermediate imine prior to addition of the borohydride resin since the aldehyde would otherwise be cleanly reduced to the corresponding alcohol. Following reduction of the imine,[10] the excess amine was removed by addition of benzaldehyde resin, which selectively scavenges the excess primary amine from the secondary amine product. The products were then characterized by liquid chromatography (LC)/mass spectrometry (MS)/NMR. Twelve out of the 18 reactions proceeded in 80+% yields, five out of 18 in 50−80% yields, and one reaction failed. The principal impurities were the alcohol from aldehyde reduction and ring-opened lactam products from the reaction with excess amine.

An alternative strategy was adopted for the array of tertiary amines **14** (Scheme 2). *m*-Chloromethylbenzoyl chloride was coupled to **10** in 42% yield, and the iodide **13** was then efficiently prepared by a Finkelstein reaction. The iodide reacts much more quickly than the corresponding chloride with a secondary amine (1 h), and very little quaternary ammonium salt is generated. To scavenge the acid produced, excess amine was initially used, but subsequent removal of residual amine with scavenging isocyanate resin was capricious and required vigorous shaking. Instead, an ion exchange resin, Amberlyst A-21 (superior to Dowex MWA1 or Dowex 66), proved suitable. From control experiments, acetonitrile was preferred to DCM, tetrahydrofuran (THF), or dimethylformamide (DMF) as solvent. Eventually, we opted to use excess iodide rather than excess amine, as we had developed a rapid and simple purification process using SPE SCX cartridges (benzene sulfonic acid-derivatized silica).[11]

Scheme 3[a]

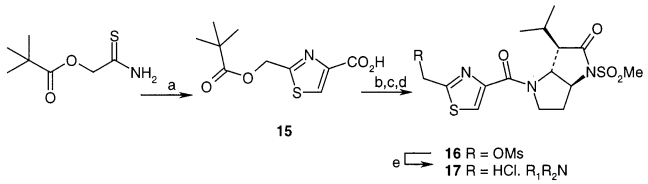

[a] All compounds racemic. Reagents: (a) $BrCH_2COCO_2H$ (1.1 equiv), EtOH, 4 Å sieves, reflux, 18 h, 68%. (b) K_2CO_3 (1.8 equiv), H_2O, MeOH, reflux, 4.5 h, 86%. (c) Compound **10**, EDC (1.1 equiv), HOBT (1.1 equiv), DMF, room temperature, 4 h, 76%. (d) $MeSO_2Cl$ (1.7 equiv), Et_3N (1.9 equiv), CH_2Cl_2, room temperature, 5 h, 38%. (e) Mixture of secondary amines (0.67 equiv in total), Et_3N (2 equiv), CH_2Cl_2, room temperature, 2 d, and then workup and 1 M HCl in Et_2O, EtOAc, and then trituration with Et_2O.

Using this process in a 96 well plate in a HiTOPS block, with a set of 80 amines selected on the basis of diverse lipophilicity and CMR, we prepared 73 tertiary amines of general structure **14** in yields of 10−96%. The seven amines that failed were all very hindered (e.g., diisopropylamine and dicyclohexylamine). Over 80% of the amines were prepared in at least 70% yield. All of the products were characterized by LC/MS and some by LC/MS/NMR.

6.2. SAR. We prepared large numbers of benzylamines with varying substitution patterns principally because they were among the most potent examples in the HWB assay (33% of examples were <0.5 μM in HWB). Most were also potent against isolated elastase (>50% of examples were <50 nM). However, in this series, the majority of these compounds were metabolically labile as determined by high turnover in hamster liver microsomes and low plasma concentrations in the dog cassette. We were unable to resolve these shortcomings in this series.

7. Thiazoles. 7.1. Mixtures of Thiazoles for Cassette Dosing. After a reasonable number of compounds were synthesized and screened, we found the most discriminating assay to be the measurement of the clearance in the dog cassette. Typically, discrete compounds were synthesized, evaluated in the in vitro assays, and then mixed for the cassette study. It occurred to us that it might be more efficient to initially prepare a mixture, prioritize which compounds were cleared more slowly in a cassette study, and then synthesize a much smaller subset as discrete compounds for further evaluation.

In general, the plasma clearance of each component compound of any cassette mixture was estimated by comparison of its initial concentration with the concentration at various timepoints, as judged by MS. The implication of this is that the initial concentrations of the component compounds do not have to be the same. This meant that neither a uniform molar ratio of the component compounds nor a precise determination of the molar ratio was required.

2-(*tert*-Butylcarbonyloxy)thioacetamide and bromopyruvic acid were condensed to give the thiazole **15** in 68% yield (Scheme 3). Hydrolysis of the pivalic ester followed by coupling to the *trans*-lactam **10** proceeded smoothly. The mesylate **16** was then prepared in 38% yield in the usual fashion; it proved to be a stable, crystalline intermediate. The next step was alkylation of **16** with our mixture of amines. To avoid the possibil-

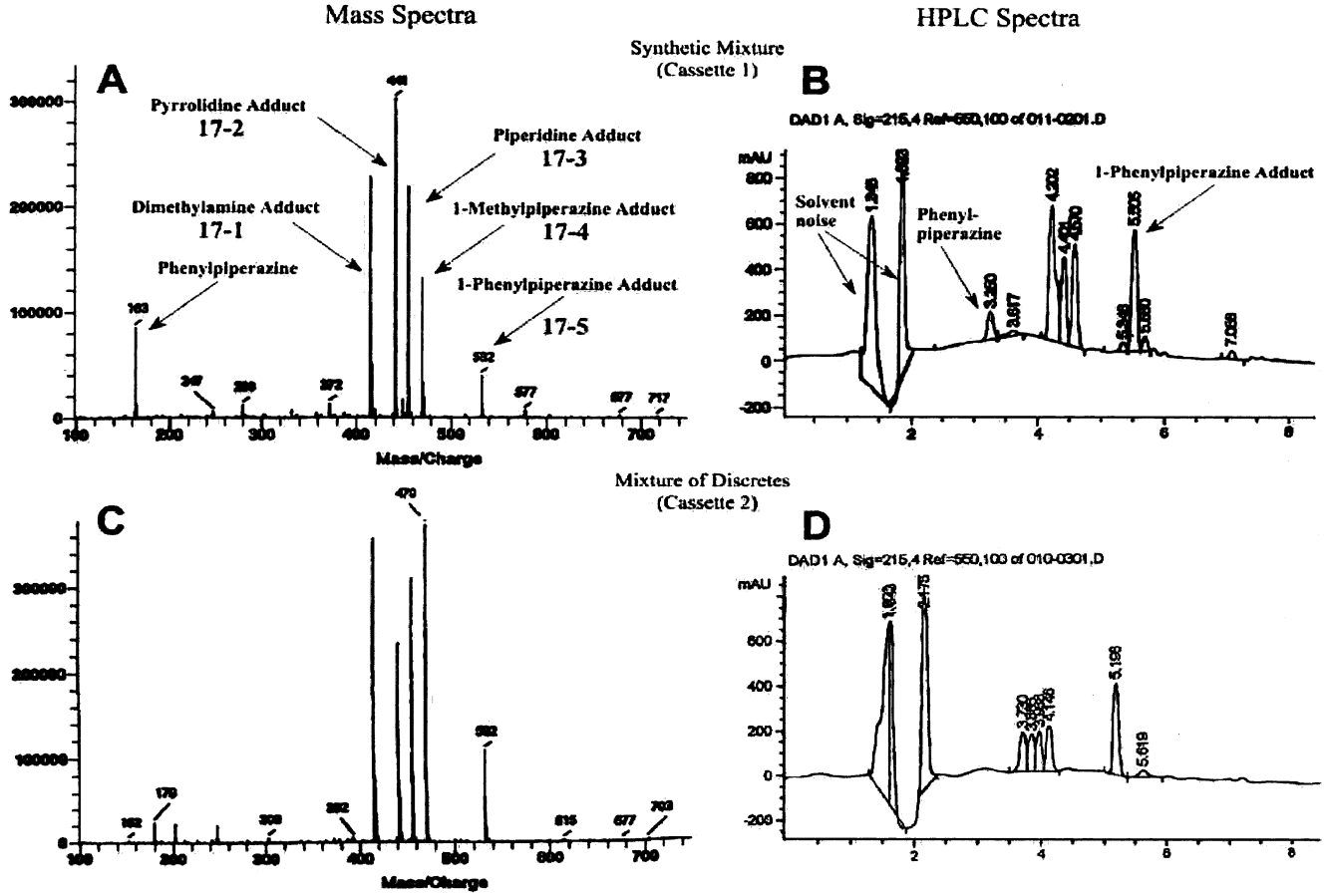

Figure 3. Mass spectra (A and C) and HPLC chromatographs (B and D) for the synthetic mixture **17** (A and B) and the mixture of discretes (C and D). Peaks corresponding to each component of the mixture are present in both sets of spectra. Note for the synthetic mixture: the presence of unreacted phenylpiperazine and the corresponding relative decrease in peak height in the HPLC for the phenylpiperazine analogue **17-5**.

ity of dialkylation of primary amines, we selected five secondary amines each with differing molecular weights to facilitate mass spectroscopic analysis (dimethylamine, pyrrolidine, piperidine, 1-methylpiperazine, and 1-phenyl piperazine). A 50% excess of mesylate **16** (with respect to the total number of moles of amine) was treated with an equimolar ratio of dimethylamine, pyrrolidine, piperidine, methylpiperazine, and phenylpiperazine in dichloromethane with triethylamine as an acid scavenger. At the end of the reaction, the solution was washed with aqueous bicarbonate and water, dried, and concentrated. The residue now contained the products, unreacted mesylate, and side products formed by decomposition of the mesylate in solution (formation of quaternary ammonium salts was very slow under these conditions). This residue was then dissolved in ether and treated with hydrogen chloride leading to precipitation of the hydrochlorides. Trituration with ether then allowed removal of the unreacted mesylate and nonbasic side products. The LC/MS analysis (Figure 3, spectra A and B) shows the presence of each compound in mixture **17**; however, the reaction with phenylpiperazine was only partially complete as indicated by the presence of peaks for the phenylpiperazine adduct **17-5** and unreacted phenylpiperazine. Comparison of the spectra A and B (Figure 3) for the synthetic mixture with the spectra C and D (Figure 3) for the mixture of discretes shows an excellent correlation. (The retention time differences in the high-performance liquid chromatography (HPLC) spectra B and D are due to solvent noise and interference.)

Table 1. Plasma Concentrations at 1 h (Relative to the Standard **2**) of Synthetic Mixtures and Mixtures of Discretes and Results from a Third Cassette, Which Included **17-2** and **17- 5**

		plasma concns[a]		
	amine	cassette 1 synthetic mixture	cassette 2 mixture of discretes	cassette 3[b]
17-1	Me_2N	1.2	1.0	
17-2	pyrrolidine	0.5	0.4	0.4
17-3	piperidine	0.3	0.2	
17-4	1-methylpiperazine	1.2	0.9	
17-5	1-phenylpiperazine	0.8	0.3	0.9

[a] Plasma concentrations relative to the standard **2** at 1 h. [b] Cassette 3 included **17-2**, **17-5**, and eight other compounds (structure and data not included).

The results from evaluation of the synthetic mixture **17** in the cassette (cassette 1) are in good agreement with those from an equimolar mixture of the same compounds, which had been prepared and purified as discretes (cassette 2) (Table 1). The exception is the phenylpiperazine analogue **17-5** where the relative plasma concentrations at 1 h for the synthetic mixture is 0.8 as compared with 0.3 for the mixture of discretes. From the analytical data (Figure 3), it is known that there was less of this compound present in the synthetic mixture. However, when the phenylpiperazine **17-5** was

Scheme 4[a]

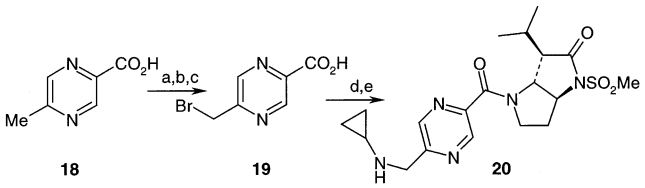

[a] All compounds racemic. Reagents: (a) MeOH, concentrated HCl, room temperature, 20 h, 70%. (b) NBS (1.0 equiv), $(BzO)_2$ (0.37 equiv), hν, CCl_4, reflux, 5 h, 26%. (c) KOH (10 equiv), H_2O, room temperature, 2 h, 68%. (d) Compound **10** (0.7 equiv), EDC (1.2 equiv), MeCN, room temperature, 20 h, 50%. (e) Cyclopropylamine (6 equiv) (see ref 12), NaI (1.5 equiv), K_2CO_3 (6 equiv), CH_2Cl_2, room temperature, 1−3 d, 63%.

included as a component of a mixture of discretes in a third cassette experiment (cassette 3), the relative plasma concentration was 0.9. It is apparent that the original value for the mixture of discretes was inaccurate rather than the value from the synthetic mixture (cf. the values for the pyrrolidine derivative **17-2** across all three cassettes). This illustrates the point made above that precise equimolar mixtures are not necessary using this process. Having validated this protocol, we subsequently prepared two further series of novel thiazoles as synthetic mixtures (without preparing them as discretes) for evaluation in the cassette.

7.2. SAR from the Thiazoles. Over two-thirds of the thiazoles prepared inhibited HNE with IC_{50} values of <20 nM, and half had IC_{50} values <0.5 μM in HWB. However, the vast majority of the more potent thiazoles in this series proved to have high turnover in hamster liver microsomes and/or low plasma concentrations in the dog cassette experiments. The few compounds evaluated in vivo in hamster were mediocre.

8. Pyrazines, Azetidines, and Oxazoles. 8.1. Array Preparations: Pyrazines. Synthesis of an array of pyrazine analogues (which have a predicted clog*D* of over 2 log units lower than the corresponding benzene derivatives) was straightforward (Scheme 4). The commercially available pyrazine acid **18** was esterified and brominated under photolytic conditions to give the mono bromide in 26% yield together with 22% of the α,α-dibromide. After ester hydrolysis, the bromo-acid **19** was coupled to **10** and the array was prepared by treatment with either the secondary amines[12] and sodium iodide in dichloromethane or the amine hydrochlorides, sodium iodide, and potassium carbonate in dichloromethane. Exemplified here is the cyclopropyl derivative **20** prepared in 63% yield.

8.2. Array Preparations: Azetidines. The preparation of the azetidine array commenced from 3-azetidinecarboxylic acid (Scheme 5). Protection of the azetidine *N* as its benzylcarbamate allowed efficient coupling with **10** in excellent yield. Removal of the benzyl carbamate is best achieved by hydrogenolysis in acetic acid using platinum oxide as catalyst. Hydrogenolysis with palladium hydroxide as catalyst gives complex mixtures. Reductive amination with the amine **21** as its acetate with a range of aldehydes, followed by formation of the hydrochlorides, gave the products in moderate to good yield[13] (exemplified for the neopentyl derivative **22**).

8.3. Array Preparations: Oxazoles. The oxazole ring system was prepared using standard procedures[14] from ethyl acetimidate and serine methyl ester (Scheme 6) followed by oxidation. The resulting oxazole **23** sublimes readily. Bromination[15] of the methyl group gave mixtures of starting material, α,α-dibromo material, and the monobromo product **24** in low to moderate yields. Originally, we had wished to couple the corresponding bromo-acid to the lactam **10**; unfortunately, attempted hydrolysis of **24** under basic or acidic conditions gave complex mixtures. However, in an array format, reaction of **24** with secondary amines[16] followed by basic hydrolysis, conversion to the acid chloride, and coupling with **10** proceeded to give the target amines in fair to good yields.[17] The pyrrolidine derivative shown here was prepared using this sequence in 45% yield.

8.4. Pyrazines, Azetidines, and Oxazoles: SAR. The most striking feature of the SAR of the pyrazines, azetidines, and oxazoles was that only one example emerged from each array as a potential candidate having the desired profile: **20**, **22**, and **25**. While the pyrazines as a class were extraordinarily potent vs HWB, with 80% having IC_{50} values <0.5 μM, only the cyclopropylamine derivative **20** emerged with acceptable clearance and efficacy in the in vivo hamster assay. Most of the azetidines and oxazoles failed on potency grounds either against isolated HNE or in HWB. Only the neopentyl-azetidine **22** and pyrrolidine-oxazole **25** have the desired profile.

8.5. Syntheses of Enantiomerically Pure Candidates. From the biological evaluation of the above series, the racemates **20**, **22**, and **25** were selected for further study. Our first task was to prepare large quantities of these compounds in enantiomerically pure form.

8.5.1. Preparation of the Enantiomerically Pure Pyrazine 28 and Azetidine 29. To reduce the cost of synthesis, we wanted to streamline the processing of the costly enantiomerically pure *trans*-lactam moiety **27** (Scheme 7).[5] We therefore chose to couple the *trans*-lactam to a cyclopropylamine-derived pyrazine acid. In a three step sequence, the pyrazine acid **18** was first brominated to give a mixture of mono and α,α-dibromo acids. After workup, this crude mixture was treated with cyclopropylamine. This amine only reacts with the monobromide. The desired cyclopropylaminopyrazine acid was then extracted into dilute hydrochloric acid, which was then basified with sodium hydroxide and reacted with di-*tert*-butyl dicarbonate to furnish the *tert*-butyl carbamate **26** in 13% yield for the three steps. Conditions for coupling this acid **26** to the *trans*-lactam **27**, which worked both on a large and a small scale, were eventually found with the use of *O*-(7-azabenzotriazol-1-yl)-*N*,*N*,*N*′,*N*′-tetramethyluronium hexafluorophosphate (HATU) in acetonitrile. This proceeded in 89% yield on a 20 g scale. Deprotection of the carbamate and hydrochloride formation were achieved with hydrogen chloride in dioxan. Recrystallization from water-2-propanol gave **28** in greater than 99% purity as judged by HPLC. The enantiomerically pure neopentyl-azetidine **29** was prepared using the enantiomerically pure *trans*-lactam **27** via the same route as that described (Scheme 5).

8.5.2. Preparation of the Enantiomerically Pure Oxazole 32. The synthesis used for the racemic pyrrolidine-oxazole **25** (Scheme 6) involved a low-yielding

Scheme 5[a]

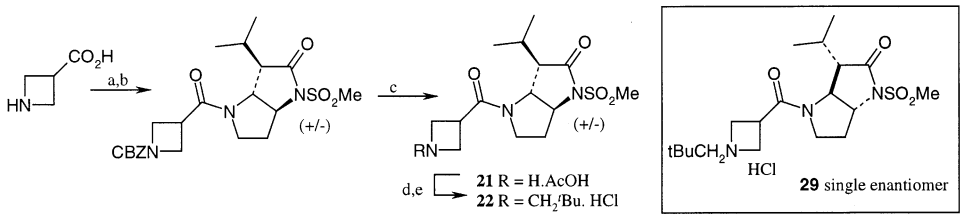

[a] Reagents: (a) CBZCl (1.05 equiv), 0.5 M K_2CO_3, dioxan, room temperature, 18 h, 92% crude. (b) Compound **10**, EDC (1.2 equiv), 5:1 CH_2Cl_2:MeCN, room temperature, 7 h, 97% crude. (c) 5% PtO_2, H_2, AcOH, room temperature, 8 h, 98% crude. (d) *t*-BuCHO (2 equiv), $Na(AcO)_3BH$ (2 equiv), trace AcOH, CH_2Cl_2, room temperature, 18 h, 73%. (e) 1 M HCl in Et_2O, CH_2Cl_2 86%.

Scheme 6[a]

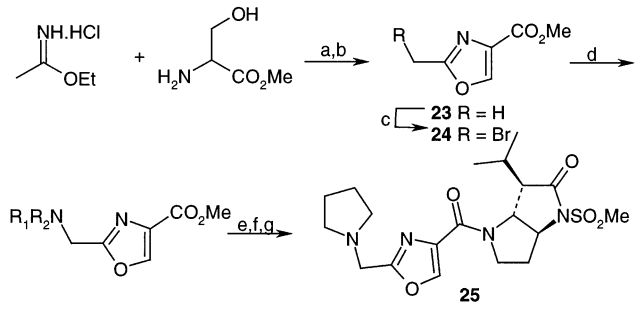

[a] All compounds racemic. Reagents: (a) Et_3N (1 equiv), CH_2Cl_2, reflux, 5.5 h, 77%. (b) DBU (0.25 equiv), CCl_4:pyridine:MeCN (1.2:1.8:2.3), room temperature, 18 h, 65%. (c) NBS (1.1 equiv), $(PhCO_2)_2$ (0.05 equiv), CCl_4, hν (200 W tungsten lamp), reflux, 1.5 h, 15−34%. (d) Pyrrolidine (1.1 equiv), K_2CO_3 (1.5 equiv), MeCN, room temperature, 6−48 h, see 17 for other amines. (e) NaOH (3 equiv), H_2O, dioxan, room temperature, 5 h. (f) $(COCl)_2$ (5 equiv), DMF (catalytic), CH_2Cl_2, room temperature, 1.5 h. (g) Compound **10** (0.8 equiv), $NaHCO_3$ (4 equiv), CH_2Cl_2, room temperature, 4 h, 45% (see ref 17 for yields of other amines); purify then 1 M HCl in Et_2O (1.1 equiv), CH_2Cl_2, quantitative.

Scheme 7[a]

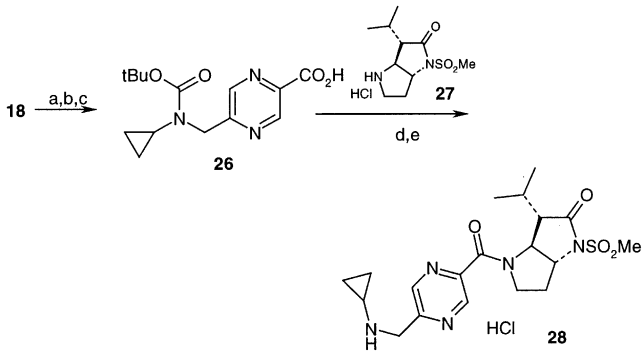

[a] Reagents: (a) Br_2 (1.1 equiv), AcOH, 80 °C, 1 h. (b) Cyclopropylamine (2.0 equiv), Et_3N (1.0 equiv), room temperature, 20 h. (c) Boc_2O (1.2 equiv), 1,4-dioxan, room temperature, 44 h, 13% for three steps. (d) Compound **27** (1 equiv) (see ref 5), HATU (1.1 equiv), DIPEA (2.0 equiv), MeCN, room temperature, 2 h, 89%. (e) 4 M HCl, 1,4-dioxan, room temperature, 2 h, and then recrystallize from 5% H_2O in ^{i}PrOH (82%).

bromination, which was not amenable on a large scale. An alternative multigram process featuring a rhodium-catalyzed insertion reaction was thus developed.[18] Ethyl diazoacetate was formylated with the Vilsmeier reagent to afford, after hydrolysis, the aldehyde **30** in 73% yield (Scheme 8). Treatment of **30** with catalytic rhodium acetate generated the carbene, which was reacted with bromoacetonitrile[19] to afford the oxazole **31** in 38% yield after chromatography. This oxazole was then readily converted into **32** by treatment with pyrrolidine, saponification of the ester, and coupling with **27** using EDC in the presence of hydroxybenzotriazole. After the hydrochloride was formed, recrystallization from acetone gave analytically pure **32** in 65% yield.

Scheme 8[a]

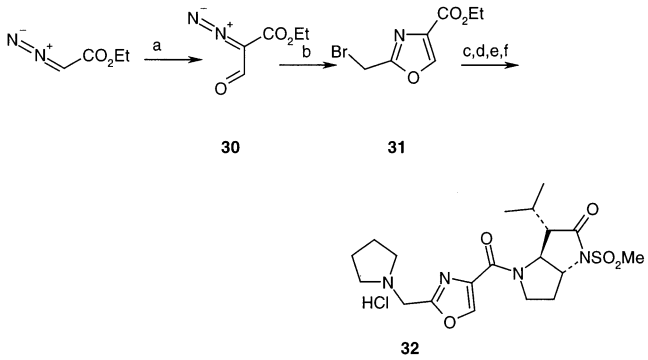

[a] Reagents: (a) $ClCHNMe_2 + Cl^-$ (0.5 equiv), $CHCl_3$, −5 to 20 °C, 3 h, and then 10% AcOH in H_2O, room temperature, 3 h, 73%. (b) $BrCH_2CN$ (as solvent), $Rh_2(OAc)_4$ (1.5 mol %), 75 °C, 8 h, 38%. (c) Pyrrolidine (3.0 equiv), MeCN, room temperature, 45 min, 57%. (d) K_2CO_3 (1.0 equiv), EtOH, H_2O, reflux, 4 h. (e) Compound **27** (1 equiv), EDC (2 equiv), HOBT (1 equiv), MeCN, room temperature, 20 h. (f) 1 M HCl in Et_2O (1.1 equiv), room temperature, 15 min and then recrystallized from Me_2CO, 65% for two steps.

Table 2. Kinetic Parameters Measured at pH 7.4[a]

inhibitor	$k_{obs}/[I]$	k_{on} (s^{-1} M^{-1})	k_{off} ($\times 10^{-6}$ s^{-1})	K_i (nM)[b]	$t_{1/2}$[c] (h)
1 GW311616	757	6630	2.07	0.31	93
28 GW447631	28 735	251 668	3.53	0.014	54.5
29 GW469002	720	6306	10.9	1.73	17.6
32 GW475151	3483	30 505	4.85	0.16	39.7

[a] HNE (3.4 nM) was assayed with 1 mM of the chromogenic substrate MeOSuc-AAPV-*p*NA (Sigma, M4765) at 30 °C in 0.1 M Hepes (pH 7.4), 0.3 M NaCl, 10% (v/v) DMSO, and 0.03% (v/v) TritonX-100 containing 0−1 μM inhibitor. See refs 21 and 22 for further details. [b] $K_i = k_{off}/k_{on}$, k_{off} and k_{on} are, respectively, the dissociation and association rate constants.[22] [c] $t_{1/2} = 0.693/k_{off}$ represents the half-life time of the acyl-enzyme.

9. Summary of Potency and In Vitro and In Vivo Data. The previous section highlights the use of recent chemical technologies in our medicinal chemistry program. Emerging from the large number of derivatives that were prepared were three that satisfied our criteria for back-up candidates. These were the cyclopropylpyrazine **28** (GW447631A),[20] the neopentylazetidine **29** (GW469002A),[21] and the pyrrolidinyloxazole **32** (GW475151A),[21] which represent a diverse set of side chains. (For further details on the biological activity of many of these derivatives, see refs 20 and 21.)

Table 2 compares the kinetic parameters determined for the three potential back-up compounds with those for **1** (GW311616A). In each case, the acylated enzyme

Table 3. Biological Profiles of the Back-Up Compounds[a]

parameter	**1** GW311616	**28** GW447631	**29** GW469002	**32** GW475151
HNE IC_{50} (μM)[b,c]	0.022	0.011	0.037	0.010
		Selectivity Assays IC_{50} (μM)		
chymotrypsin[b,d]	4.2	0.54	31	3
trypsin[b,e]	>100	>100	>100	>100
cathepsin G[b,d]	>100	>100	>100	>100
		Whole Blood IC_{50} (μM)[c]		
human	0.67	0.15	0.19	0.25
dog	0.35	0.26	0.17	0.39
		Hamster In Vivo[c] (% Elastase Inhibition at 2.2 mg/kg po)		
bronchoalveolar lavage	81	90	83	93
bone marrow	48	69	56	65
		Dog In Vivo[c] (% Elastase Inhibition in Peripheral Blood at 2 mg/kg po)		
6 hours	100	99	99[f]	100
3 days	97	92	92[f]	100

[a] For comparison of values for **1** with literature compounds, see ref 4. [b] Values represent a mean of three experiments. All values are within 30% of the mean. These values are after 15 min of preincubation. [c] See Experimental Section for practical details. [d] See ref 2 for experimental details. [e] See ref 22 for experimental details. [f] Dose level was 1.1 mg/kg po.

dissociates very slowly, so that the inhibitors behave essentially irreversibly. Compound **28** is particularly potent, having a picomolar K_i value. As with **1**, selectivity against other serine proteases has been maintained (Table 3), and these new compounds are even more potent than the original lead in the HWB assay, demonstrating inhibition of intracellular elastase. Potent inhibition was also shown in the analogous dog whole blood assay.

This potency was maintained in vivo after oral dosing in both hamsters and dogs (Table 3). In the hamster, inhibition of intracellular elastase in neutrophils recovered by bronchoalveolar lavage is thought to reflect inhibition within cells in the circulation. These cells have then been recruited to the lung with IL-8. Inhibition in the bone marrow, on the other hand, is believed to give rise to prolonged duration of action of the compounds, since any neutrophils released into the circulation would already have their complement of elastase inhibited. (The level of inhibition in the bone marrow is lower than that in bronchoalveolar lavage in each case.) This hypothesis is supported by the dog data (Figure 4) and suggests a common mechanism between the species. At the lowest dose of compound (0.22 mg/kg), elastase inhibition in circulating neutrophils rapidly reaches greater than 50% but has returned to control values by 24 h. At the 2 mg/kg dose level, elastase activity is virtually eliminated for at least 5 days. At the intermediate dose, inhibition is between the two. Each of the three back-up compounds was potent in vivo.

10. Pharmacokinetics (See Table 4). All four compounds **1**, **28**, **29**, and **32** exhibit high plasma clearance in rat, which equates to or exceeds liver blood flow (69−225 mL/min/kg). These clearances combined with the moderate to high volumes of distribution (2.6−7.5 L/kg) result in short plasma half-lives of less than or equal to 1 h. Despite the high clearance observed with these compounds, oral bioavailability ranging from 24 to 60% is evident, which suggests that clearance is predominantly extrahepatic. While the pharmacokinetics of the compounds studied are broadly similar, the plasma clearance of **28** is approximately 3-fold higher than the other inhibitors and the oral exposure

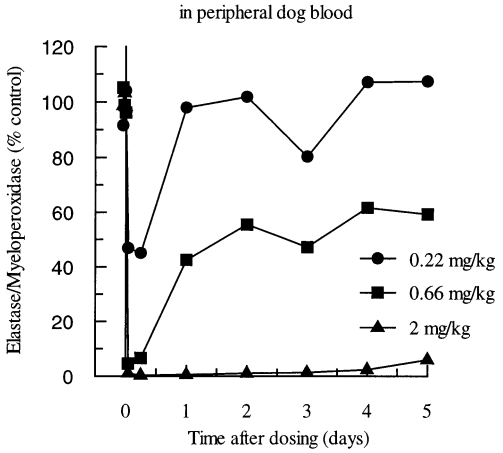

Figure 4. Effect of orally dosed **32** (GW475151) on intracellular elastase in peripheral dog blood. Elastase and myeloperoxidase activities were determined in lysed white cells from peripheral blood (2 dogs/dose level). Ratios were compared with the mean of three predose samples for each dog.

is notably lower. As an oral therapy, it is therefore considered to be pharmacokinetically inferior to the other compounds.

The pharmacokinetic profile in the dog broadly reflects that seen in the rat with clearance values that approach/exceed liver blood flow (23−50 mL/min/kg), moderate volumes of distribution (1.9−3.5 L/kg), and short plasma half-lives of typically less than 2 h. The oral bioavailability again suggests that clearance is predominantly extrahepatic, and the data (two dogs per compound) shows that essentially complete oral bioavailability is achieved with all four compounds. However, as evident in the rat, the oral exposure of **28** is lower than that of the other three compounds and its plasma clearance is higher. Therefore, on the basis of its pharmacokinetic profile in both the rat and the dog, this compound is considered to be inferior to the other elastase inhibitors studied.

11. Cocrystal Structure of HNE with 32 (GW475151). The X-ray crystal structure of **32** in a complex with HNE at pH 4.0 has been determined at 2.0 Å resolution. The electron density that covers the whole of the inhibitor molecule provides a clear basis

Table 4. Pharmacokinetic Parameters of **1** (GW311616A),[a] **28** (GW447631A),[a] **29** (GW469002A),[a] and **32** (GW475151A)[a] from iv and po Dosing in Rat at 2 mg/kg and Dog at 0.66 mg/kg

	1 (GW311616A)				**28** (GW447631A)				**29** (GW469002A)				**32** (GW475151A)			
	rat		dog[b]		rat[c]		dog		rat		dog		rat		dog	
param	iv	po	iv	po	iv	po	iv	po	iv	po	iv	po	iv	po	iv	po
C_{max} (ng/mL)		232		152		135		205		142		130		147		138
T_{max} (h)	0.05	0.5		0.7	0.03	0.25		0.25	0.03	0.75		0.9	0.03	0.25	0.03	0.5
AUC∞ (ng/mL h)	424	263	405	430	148	64	220	147	482	217	488	417	392	93	286	308
$T_{1/2}$ (h)	1.1	0.8	1.5	1.6	0.3	0.4	0.4	0.4	0.8	1.2	1.8	2.1	0.4	1.3	1.0	1.4
Clp (mL/min/kg)	79		28		225		50		69		23		85		39	
V_d area (L/kg)	7.5		3.5		5.0		1.9		4.9		3.5		2.6		3.4	
F (%)		60		∼100		43		50−120		45		90		24		∼100

[a] All of the data were gathered on the hydrochlorides. [b] The **1** dog data were normalized from a 2 to 0.66 mg/kg dose. [c] The **29** rat data were normalized from a 2.4 to 2 mg/kg dose.

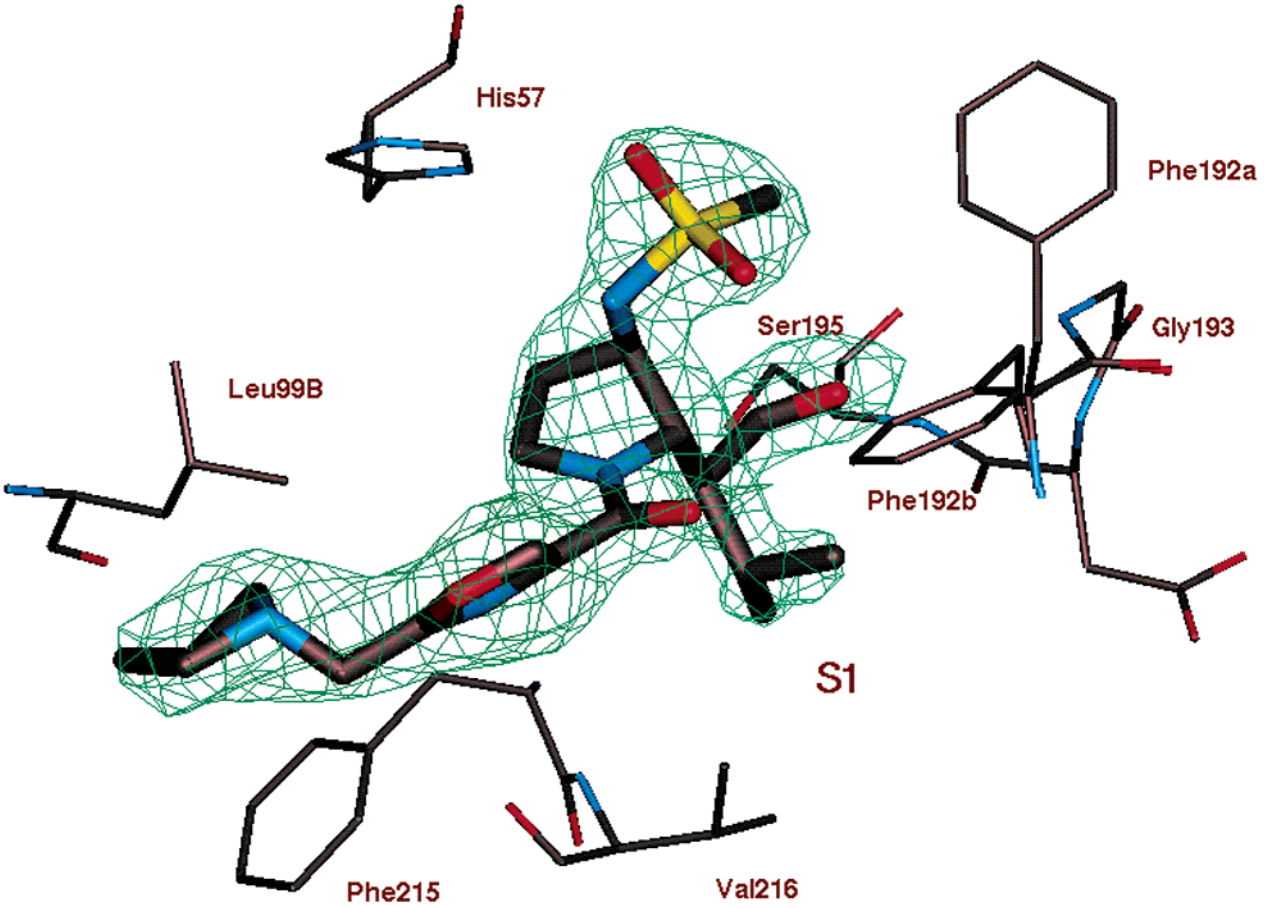

Figure 5. Crystal structure of HNE complexed with GW475151. The ring-opened ligand covalently linked to Ser195 is shown in thick bonds with the electron density of the omit map in a green/blue chicken wire net representation. Key residues of HNE are drawn in thin bonds with residues numbered as for chymotrypsin. S1 is the primary enzyme specificity pocket. The alternative positions for the side chain of Phe215 are denoted "a" and "b".

for interpretation of ligand interactions within the active site (Figure 5). The ring-opened *trans*-lactam is covalently bonded to Ser195; the S1 pocket is occupied by the isopropyl group while the ester carbonyl of the inhibitor points toward the main chain nitrogen atoms of Gly193 and Ser195 (the oxyanion hole), but distances are too long for good hydrogen bonding. His57 is displaced from its catalytic position and is replaced by two water molecules; this will contribute to the stability of the complex. The pyrrolidine group makes hydrophobic contacts with both Phe215 and Leu99B. All residues of the active site and binding pocket match closely for the two independent molecules in the asymmetric unit of the crystal apart from the side chain of Phe192. This group makes contact with the methylsulfonamide group of the inhibitor and has alternate conformations (both shown in Figure 5), which arise from differences in intermolecular contacts within the crystal. As compared with the structure of HNE in complex with a chloromethyl ketone inhibitor (1HNE),[23] the loop containing residues Val99, Asn99A, Leu99B, and Leu100 is displaced by up to 1 Å in the main chain. This probably occurs as a consequence of the hydrophobic contact between the pyrrolidine group of the ligand and the side chain of Leu99B, which moves ∼1.5 Å.

A comparison with the binding of **1** to porcine pancreatic enzyme (PPE)[5] indicates significant differences (Figure 6). Although the methylsulfonamide groups are essentially superimposed, the ring-opened lactam is

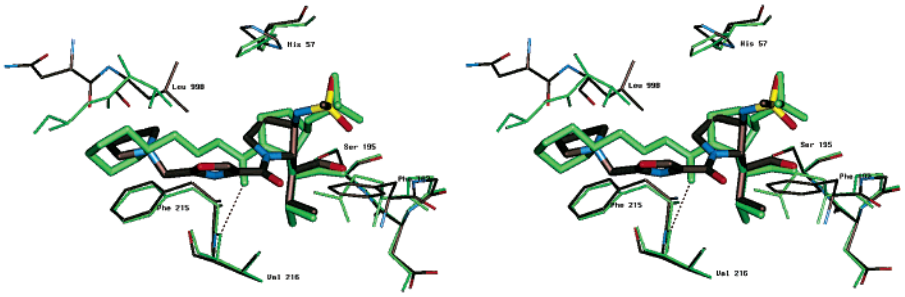

Figure 6. Stereoview of the superposition of the active site residues of the HNE−GW475151 complex (atom colors) with that of the porcine pancreatic elastase−GW311616 complex (green). The difference in the orientation of the ring-opened lactam leads to a marked shift in the pendant atoms with the loss of the hydrogen bond from the carbonyl to the main chain NH of residue Val 216. Labeled residues are those of the HNE complex.

rotated anticlockwise relative to **1**, bringing the inhibitor chain down and out in the pocket. As a consequence, there is no hydrogen bond from the carbonyl of the ligand to the main chain NH of residue 216; instead, this group points out into solvent.

12. Conclusion. Described here is the strategy and discovery of three back-up candidates to **1**, which are suitable for development. We successfully improved HWB potency and with **29** and **32** maintained acceptable clearance rates in rat and dog. Through the use of modern array techniques, we were able to prepare rapidly a substantial number of compounds for biological evaluation. Evaluation of clearance using the dog cassette protocol allowed 136 compounds to be screened in 7 months of which 94 were screened in 2 months, demonstrating its value.

Experimental Section

For descriptions of equipment and techniques, see refs 2 and 5. For the preparative details of array and library compounds, see refs 20 and 21. For descriptions of assay conditions, refer to the published procedures cited in the references.

Preparation of 28. 5-[(*tert*-Butoxycarbonyl-cyclopropyl-amino)methyl]pyrazine-2-carboxylic Acid 26. Bromine was added to a stirred suspension of 2-methylpyrazin-5-carboxylic acid (60 g) in acetic acid (300 mL). The reaction mixture was then heated to 80 °C for 1 h. The solvent was evaporated in vacuo, and the residue was partitioned between ethyl acetate (250 mL) and 2 M aqueous HCl (250 mL). The aqueous phase was extracted with further ethyl acetate (5 × 250 mL), the combined organics were washed with 2 M HCl (100 mL) and saturated brine solution (100 mL), dried ($MgSO_4$), and filtered, and the solvent was evaporated in vacuo to leave a brown solid. The solid was stirred in acetonitrile (900 mL), and triethylamine (60 mL) and cyclopropylamine (30 mL) were added. After the mixture was stirred for 20 h at room temperature, further cyclopropylamine (30 mL) was added and the mixture was stirred for a further 15 min. The volatiles were evaporated in vacuo, and the residue was partitioned between ethyl acetate (200 mL) and 2 M aqueous HCl (300 mL). The organic phase was extracted with further 2 M HCl (4 × 200 mL), and the combined aqueous extracts were washed with ethyl acetate (50 mL), cooled in an ice bath, and basified with 10 M aqueous sodium hydroxide (120 mL). The solution was washed with ethyl acetate (3 × 200 mL) and diethyl ether (200 mL), and remaining organic volatiles were removed in vacuo to give a brown aqueous solution. To the solution was added 1,4-dioxane (500 mL) and di-*tert*-butyl dicarbonate (71 g), and the mixture was stirred at room temperature for 20 h. Further di-*tert*-butyl dicarbonate (10 g) was added, and stirring was continued for a further 24 h. Citric acid (85 g) was added to the stirred mixture before it was extracted with ethyl acetate (2 × 200 mL + 3 × 150 mL + 2 × 100 mL). The combined extracts were dried ($MgSO_4$) and filtered, and the solvent was removed in vacuo to give a brown oil, which was purified by flash column chromatography on silica (Merck 9385), with 100:8:1 dichloromethane/methanol/acetic acid as the eluent. The required fractions were evaporated to dryness in vacuo to give a tan-colored solid, which was stirred vigorously in 5:1 cyclohexane/diethyl ether until finely divided. The solid was filtered off and dried in vacuo to give the title compound as an orange/brown solid (16.65 g). TLC (100:8:1 dichloromethane/methanol/acetic acid) $R_f = 0.31$. MS MH^+ (found) 294, MH^+ (calcd) 294.

Cyclopropyl-[5-(6*S*-isopropyl-4-methanesulfonyl-5-oxo-hexahydro-(3a*R*,6a*S*)-pyrrolo[3,2-b]pyrrole-1-carbonyl)-pyrazin-2-ylmethyl]carbamic Acid *tert*-Butyl Ester. Compound **27**[5] (11.36 g), **26** (13.53 g), and *O*-(7-azabenzotriazol-1-yl)-*N*,*N*,*N*′,*N*′-tetramethyluronium hexafluorophosphate (19.3 g) were stirred in acetonitrile (260 mL) at room temperature, and *N*,*N*-diisopropylethylamine (16 mL) was added. After the mixture was stirred for 2 h, the solvent was removed in vacuo, and the residue was diluted with dichloromethane (250 mL) and washed with 1 M sodium carbonate solution (250 mL). The aqueous phase was extracted with dichloromethane (3 × 150 mL). The combined organics were washed with 1 M sodium carbonate solution (50 mL), dried ($MgSO_4$), filtered, and the solvent was evaporated in vacuo to leave a yellow-brown solid. The solid was purified by flash column chromatography (Merck 9385 silica) using 50% ethyl acetate/cyclohexane as eluent, and the required fractions were evaporated to dryness in vacuo to give the title compound as a white foam (21.55 g); $[\alpha]_D^{20}$ +69.5° (c = 0.8, MeCN). MS MH^+ (found) 522, MH^+ (calcd) 522.

(3*S*,3a*S*,6a*R*)-4-(5-Cyclopropylaminomethyl-pyrazine-2-carbonyl)-3-isopropyl-1-methanesulfonyl-hexahydro-pyrrolo[3,2-b]pyrrol-2-one Hydrochloride 28. A solution of cyclopropyl-[5-(6*S*-isopropyl-4-methanesulfonyl-5-oxo-hexahydro-(3a*R*,6a*S*)-pyrrolo[3,2-b]pyrrole-1-carbonyl)pyrazin-2-ylmethyl]carbamic acid *tert*-butyl ester (21.53 g) and 4.0 M HCl in 1,4-dioxan (200 mL) was stirred at room temperature for 2 h. The solvent was removed in vacuo to give an off-white solid. The solid was recrystallized from hot 5% water/2-propanol (2.3 L) to give **28** (15.54 g) as a white solid; mp 183−185 °C; TLC (Silica, eluent 200:8:1 dichloromethane:ethanol:0.880 ammonia) $R_f = 0.21$; $[\alpha]_D^{20}$ +51.3° (c = 0.9, 1:1 H_2O/MeCN). CD: λ_{max} 250.2 nm (ΔE −1.34 M^{-1} cm^{-1}), λ_{max} 285.4 nm (ΔE +0.99 M^{-1} cm^{-1}), (MeCN/H_2O). ^1H NMR (DMSO-d_6, 400 MHz): δ 9.80 (bs, 2H), 9.04 (s, 1H), 8.88 (s, 1H), 4.56 (s, 2H), 4.03−3.83 (m, 3H), 3.62 (t, J = 11 Hz, 1H), 3.32 (s, 3H), 3.13−3.07 (m, 1H), 2.94 (m, 1H), 2.80 (m, 1H), 2.33 (m, 1H), 2.09 (m, 1H), 1.22 (d, J = 7 Hz, 3H), 1.02 (d, J = 7 Hz, 3H), 0.93 (m, 2H), 0.76 (m, 2H). MS MH^+ (found) 422.19, MH^+ (calcd) 422.19. Anal. Found C, 47.4; H, 6.4; N, 14.3; S, 6.5; Cl, 7.8; water, 4.9%. $C_{19}H_{27}Cl\,N_5O_4S{\cdot}HCl{\cdot}1.3H_2O$ requires C, 47.4; H, 6.4; N, 14.6; S, 6.7; Cl, 7.4; water, 4.9%.

Preparation of 29. 1-Benzyloxycarbonyl Azetidin-3-oic Acid. To azetidine-3-carboxylic acid (0.50 g), potassium carbonate (0.82 g), dioxan (5 mL), and water (10 mL) was added benzyl chloroformate (0.74 mL) at room temperature, and the mixture was stirred for 6 h under nitrogen. Piperazine (5

drops) was then added. After 0.5 h, the dioxan was removed in vacuo and the residue was diluted with 2 M hydrochloric acid (25 mL). After it was extracted with ethyl acetate (35 mL), the organic layer was washed with brine (10 mL) and dried ($MgSO_4$). Solvent removal in vacuo gave the title compound as a colorless oil (1.07 g). MS MNH_4^+ (found) 253, MNH_4^+ (calcd) 253.

(3*S*,3a*S*,6a*R*)-3-(6-Isopropyl-4-methanesulfonyl-5-oxohexahydro-pyrrolo[3,2-b]pyrrole-1-carbonyl)azetidine-1-carboxylic Acid Benzyl Ester. A mixture of **27**[5] (0.90 g), 1-(3-dimethylaminopropyl)-3-ethylcarbodiimide (0.91 g), and acetonitrile (12 mL) was stirred for 5 min under nitrogen after which 1-benzyloxycarbonyl azetidin-3-oic acid (0.90 g) in acetonitrile (30 mL) was added. After 18 h, the solvent was removed in vacuo and the residue was treated with 2 M hydrochloric acid (30 mL). The mixture was extracted with ethyl acetate (90 mL). The organic layer was washed with 2 M hydrochloric acid (30 mL), saturated sodium bicarbonate solution (2 × 30 mL), and brine (30 mL), dried ($MgSO_4$), and concentrated in vacuo. The residue was purified by flash chromatography on silica (Merck 9385) eluting with 10% and then 20% acetonitrile in dichloromethane to give the title compound as a colorless foam (0.80 g). MS MH^+ (found) 464, MH^+ (calcd) 464.

(3*S*,3a*S*,6a*R*)-4-(Azetidine-3-carbonyl)-3-isopropyl-1-methanesulfonyl-hexahydro-pyrrolo[3,2-b]pyrrol-2-one Acetate. Platinum(IV) oxide (1.0 g) and acetic acid (50 mL) were prehydrogenated for 0.5 h and then (3*S*,3a*S*,6a*R*)-3-(6-isopropyl-4-methanesulfonyl-5-oxohexahydro-pyrrolo[3,2-b]pyrrole-1-carbonyl)azetidine-1-carboxylic acid benzyl ester (0.80 g) in acetic acid (50 mL) was added. After it was vigorously stirred under hydrogen for 19 h, the reaction was filtered through a 3 M Empore C18 extraction disk cartridge and concentrated in vacuo. The residual gum was dried by azeotropic distillation with toluene (3 × 50 mL), and the residue was triturated with ether (2 × 20 mL) to give the title compound as a white powder (0.63 g). MS MH^+ (found) 330, MH^+ (calcd) 330.

(3*S*,3a*S*,6*R*)-4-[1-(2,2-Dimethyl-propyl)azetidine-3-carbonyl]-3-isopropyl-1-methanesufonyl-hexahydro-pyrrolo-[3,2-b]pyrrol-2-one 29. To (3*S*,3a*S*,6a*R*)-4-(azetidine-3-carbonyl)-3-isopropyl-1-methanesulfonyl-hexahydro-pyrrolo[3,2-b]pyrrol-2-one acetate (0.625 g) in dichloromethane (90 mL) were added acetic acid (9 drops, ca. 100 μL), sodium triacetoxyborohydride (0.680 g), and pivalaldehyde (0.24 mL). After 18 h, the mixture was concentrated in vacuo and the residue was treated with ethyl acetate (90 mL). This was extracted with 1 M hydrochloric acid (3 × 30 mL), and the combined extracts were taken to pH 8 with solid sodium bicarbonate. The mixture was extracted with dichloromethane (3 × 30 mL), and the combined extracts were dried ($MgSO_4$) and concentrated in vacuo. The residue was purified by flash chromatography on silica gel (Merck 9385) eluting with 200:8:1 dichloromethane:ethanol:ammonia to afford a gum (0.466 g). The gum was dissolved in dichloromethane (20 mL), treated with 1 M hydrogen chloride in ether (5 mL), and concentrated in vacuo. Recrystallization from 7% water in 2-propanol (75 mL) gave **29** as a white powder (0.298 g); mp 194−195 °C; TLC SiO_2 (100:8:1 dichloromethane:ethanol:ammonia): R_f 0.56. ^{1}H NMR (CD_3OD, 57 °C, 400 MHz): δ 4.40 (t, 2H), 4.28 (bs, 2H), 3.88 (m, 1H), 3.83−3.71 (m, 3H), 3.59 (sextet, 1H), 3.36 (t, 1H), 3.23 (s, 3H), 3.10 (s, 2H), 3.03−2.96 (m, 1H), 2.95−2.90 (m, 1H), 2.52 (quintet, 1H), 2.12 (quintet, 1H), 1.27 (d, 3H), 1.04 (s, 9H), 1.02 (d, 3H). IR (KBr diffuse reflectance): 3479, 3415, 2966, 2608, 1738, 1661 cm^{-1}. MS MH^+ (found) 400.226259, MH^+ (calcd) 400.227004 (1.9 ppm). Anal. Found: C, 50:80; H, 7.76; N, 9.37; S, 6.97%; $C_{19}H_{33}N_3O_4S\cdot 0.8H_2O$ HC1 requires C, 50.67; H, 7.97; N, 9.33; S, 7.12%. HPLC (Inertsil ODS2-IK5, 40 °C, 215 nm, 1 mL/min, solvent A H_2O + 0.1% H_3PO_4, solvent B 95% MeCN/H_2O + 0.1% H_3PO_4, gradient 0% B for 2 min, to 100% B in 40 min, 100% B for 10 min) retention time 14.247 min. HPLC (Chiralcel OD-H, 25 °C, 215 nm, 1 mL/min, isocratic 60% EtOH in heptane) retention time 7.796 min.

Preparation of 32. 2-Pyrrolidin-1-ylmethyl-oxazole-4-carboxylic Acid Ethyl Ester. To a stirred solution of 2-(bromomethyl)oxazole-4-carboxylic acid ethyl ester (43.9 g) in acetonitrile (300 mL) was added pyrrolidine (15.7 mL). After it was stirred for 10 min, more pyrrolidine (7.8 mL) was added. After a further 30 min, the solvent was removed in vacuo to leave an orange oil. The oil was partitioned between 1 M sodium carbonate (400 mL) and dichloromethane (500 mL), and the phases were separated. The organic phase was washed with water (100 mL), dried ($MgSO_4$), filtered, and the solvent was removed in vacuo to give the title compound as an orange oil (24.0 g). MS MH^+ (found) 225, MH^+ (calcd) 225.

2-Pyrrolidin-1-ylmethyl-oxazole-4-carboxylic Acid/2-Pyrrolidin-1-ylmethyl-oxazole-4-carboxylic Acid Potassium Salt. Potassium carbonate (14.8 g) was added to a solution of 2-pyrrolidin-1-ylmethyl-oxazole-4-carboxylic acid ethyl ester (24.0 g) in ethanol (150 mL) and water (150 mL). The reaction mixture was stirred at reflux for 4 h. The solvent was removed in vacuo. The orange/brown residue was azeotroped with toluene (×3) and then dried in vacuo. The solid obtained was stirred vigorously with ether (100 mL) and filtered off before it was dried in vacuo to give a mixture of the title compound together with potassium bicarbonate as a brown solid (34.5 g). This material was used without further purification. MS MH^+ (found) 197, MH^+ (calcd) 197.

(3*S*,3a*S*,6a*R*)-3-Isopropyl-1-methanesulfonyl-4-(2-pyrrolidin-1-ylmethyl-oxazole-4-carbonyl)hexahydro-pyrrolo-[3,2-b]pyrrol-2-one Hydrochloride 32. 2-Pyrrolidin-1-ylmethyl-oxazole-4-carboxylic acid/2-pyrrolidin-1-ylmethyl-oxazole-4-carboxylic acid potassium salt (32.2 g) was added rapidly to a stirred solution of 1-hydroxybenzotriazole (13.0 g) in acetonitrile (350 mL). A solution of **27** (21.7 g)[5] and 1-(3-dimethylaminopropyl)-3-ethylcarbodiimide hydrochloride (37.0 g) in acetonitrile (70 mL) was then added, and the reaction mixture was stirred for 20 h. The solvent was removed in vacuo, and the residue was partitioned between dichloromethane (900 mL) and 1.0 M sodium carbonate solution (600 mL). The aqueous phase was separated and extracted with dichloromethane (150 mL). The combined organics were washed with brine (250 mL), dried ($MgSO_4$), and concentrated in vacuo to leave a brown solid. The solid was purified by flash column chromatography (Merck 9385 silica; eluent dichloromethane:ethanol:ammonia 150:8:1 to 135:8:1) to give a cream solid (29.3 g). The solid was dissolved in dichloromethane (150 mL) and treated with 1.0 M hydrogen chloride in ether (75 mL). The solvent was removed in vacuo to leave a solid, which was redissolved in dichloromethane (150 mL) and again treated with 1.0 M hydrogen chloride in ether (75 mL). The solvent was removed in vacuo to leave a solid, which was recrystallized from acetone to give **32** (26.3 g) as a white solid; mp 156−158 °C; TLC (Silica; dichloromethane:ethanol:ammonia 100:8:1; double elution) R_f = 0.66. ^{1}H NMR (400 MHz; DMSO-d_6): δ 8.78 (s, 1H), 4.68 (s, 2H), 4.13 (ddd, J = 11, 11, 7 Hz, 1H), 4.08 (dd, J = 11, 10 Hz, 1H), 3.80 (ddd, J = 12, 10.5, 5.5 Hz, 1H), 3.60 (m, 2H), 3.55 (dd, J = 12, 10.5 Hz, 1H), 3.31 (s, 3H), 3.20 (m, 2H), 3.03 (dd, J = 12, 2.5 Hz, 1H), 2.88 (md, J = 2.5 Hz, 1H), 2.34 (m, 1H), 2.12 (m, 1H), 1.96 (m, 4H), 1.19 (d, J = 7 Hz, 3H), 0.98 (d, J = 7 Hz, 3H). Contains 0.16 Mol % acetone. IR (KBr diffuse reflectance): ν_{max} 3633, 3474, 3149, 3102, 2956, 2882, 2668, 2576, 2475, 1747, 1709, 1639, 1634, 1567, 1442, 1380, 1347, 1161, 1146, 967, 810, 547 cm^{-1}. MS MH^+ (found) 425.186372, MH^+ (calcd) 425.185867 (error 1.2 ppm). Anal. Found: C, 48.65; H, 6.39; N, 11.41; S, 6.19; Cl, 7.13%. $C_{19}H_{28}N_4O_5S\cdot HCl\cdot 0.75H_2O\cdot 0.2Me_2CO$ requires C, 48.43; H, 6.57; N, 11.53; S, 6.60; Cl, 7.29%.

Crystallography. A 4-fold excess of **32,** GW475151, was added to HNE (Calbiochem) in 10 mM sodium acetate, pH 5.0, at a protein concentration of 10 mg/mL. Crystals of the complex grew in hanging drops containing equal volumes of protein and a precipitant solution containing 1.1−1.2 M $(NH_4)_2SO_4$ (AS), 100 mM citrate, pH 3.8−4.0, at room temperature. After they were harvested into 1.2 M AS and gradual addition of 1.0 M AS, pH 4.0, with 20% glycerol, crystals were flash-frozen in a nitrogen gas stream cooled to 100 K and stored in liquid

nitrogen for subsequent data collection. Crystallographic data collection was carried out on Station 9.6 at the Daresbury-SRS using a QUANTUM4 CCD detector system (Area Detector Systems Corporation, San Diego, CA.) and evaluated by the DENZO/SCALEPACK program package.[24] The structure was determined by molecular replacement using AmoRe[25] with coordinates of the starting model from the deposited structure *1HNE*[23] with the ligand and water molecules removed. The resulting structure, which has two molecules in the asymmetric unit of $P4_322$, was refined using cycles of REFMAC[26,27] alternating with rebuilding the structure, modeling of the ligand, and addition of solvent molecules, which was carried out with the aid of the QUANTA program (Accelrys Inc., San Diego, CA). Coordinates of the HNE-GW475151 structure have been deposited in the Protein Data Bank, ID 1h1b.

Assays. HWB Elastase Inhibition Assay. Triplicate aliquots of fresh, heparinized HWB (200 μL) were added to appropriately diluted samples (10 μL) of compounds under test. Control samples (six replicates) contained water in place of compound. Samples were mixed thoroughly by pipette and were then incubated for 30 min at 37 °C. Cold red cell lysis buffer (750 μL of 155 mM ammonium chloride, 0.12 mM ethylenediaminetetraacetic acid (EDTA), 10 mM potassium bicarbonate, pH 7.4) was then added. Tubes were capped, inverted several times, and maintained at 4 °C for 15 min, inverting every 5 min. After the tubes were centrifuged at 250*g* for 10 min at 4 °C, the resulting pelleted cells were washed. The wash was with saline (300 μL), followed by centrifugation at 100*g* for 10 min at 4 °C. Pellets were washed twice more, before resuspension of the final cell pellet in buffer (200 μL of 100 mM Tris, 300 mM NaCl, 1% (w/v) HTAB, pH 8.6). Samples were stored at −20 °C. After the samples were freeze-thawed four times, elastase activity was determined by a colorimetric assay in 50 mM Tris, 150 mM NaCl, 0.6 mM MeO-Succ-Ala-Ala-Pro-Val-*p*NA at pH 8.6, measuring the rate of increase in absorbance at 405 nm.

In Vitro Assays of HNE. Assay contents: 50 mM Tris/HCl (pH 8.6), 150 mM NaCl, and 11.8 nM purified HNE. Suitable concentrations of compound under test were diluted with water from a 10 mM stock solution in DMSO. Values above were final concentrations after the addition of substrate solution. The mixture above was incubated for 15 min at 30°C at which time the remaining elastase activity was measured for 10 min in a BioTek 340i plate-reader, after the addition of 0.6 mM MeO-succinyl-alanyl-alanyl-prolyl-valyl-*p*-nitroanilide. The rate of increase in absorbance at 405 nm was proportional to elastase activity. Enzyme activity was plotted against concentration of inhibitor and an IC_{50} was determined using curve-fitting software.

HNE Kinetics. HNE (3.4 nM) was assayed with 1 mM of the chromogenic substrate MeOSuc-AAPV-*p*NA (Sigma, M4765) at 30 °C in 0.1 M Hepes (pH 7.4), 0.3 M NaCl, 10% (v/v) DMSO and 0.03% (v/v) TritonX-100 containing 0−1 μM inhibitor. See ref 22 for further details.

Selectivity Assays. The trypsin, chymotrypsin, and cathepsin G assays were carried out essentially as described in ref 2 (chymotrypsin and cathepsin G) and ref 22 (trypsin).

In Vivo Activity of Inhibitors of HNE: Oral In Vivo Model Using IL-8-Induced Lung Infiltrates for the Assessment of Intracellular Elastase Inhibition in Hamsters. Adult hamsters (100−150 g) were randomized into groups ($n = 4$) and fasted overnight. Under gaseous anaesthetic (3% isofluorane), animals were dosed orally with 1 mL/100 g water as vehicle or containing predissolved compounds. Either at the same time, or subsequently under anaesthetic, animals were dosed intratracheally with 1 μg of recombinant human IL-8 in 100 μL of sterile saline. Six hours after IL-8 dosing, animals were sacrificed using intraperitoneal pentobarbitone. The lungs were lavaged with 2 × 2.5 mL sterile saline, and femurs were removed by dissection. Intracellular elastase was prepared from neutrophils collected by lavage and from femoral bone marrow. This was achieved by sonication of the neutrophils and centrifugation to yield intracellular granules. These were disrupted by freeze/thawing and sonication. Elastase and myeloperoxidase assays were then performed on these samples to assess the efficacy of the compounds and to normalize for neutrophil recovery.

In Vivo Activity of Inhibitors of HNE Orally in Dog. Elastase and myeloperoxidase activities were determined in lysed white cells from peripheral blood (two dogs/dose level). Ratios were compared with the mean of three predose samples for each dog.

Dog Cassette: Validation. The test set of eight compounds was administered intravenously via the femoral vein at a dose level of 0.2 mg/kg body weight per compound to a female beagle dog. Blood was sampled from the jugular vein over the time period 5 min to 24 h postdose. Plasma samples were prepared by solid phase extraction. The extracts were analyzed by HPLC and detected by single ion monitoring on a Finnigan TSQ mass spectrometer. The analytical column was a Capital Inertsil ODS3 silica 5 μm, 50 mm × 2.1 mm. The mobile phase was 0.1% formic acid in water:methanol (70:30). The flow rate was 0.4 mL/min.

Dog Cassette: Standard Assay. The set of 10 novel compounds plus the internal standard **2** was administered intravenously via the femoral vein at a dose level of 0.2 mg/kg body weight per compound to a female beagle dog. Blood was sampled from the jugular vein over the time period 5 min to 2 h postdose and analyzed as above.

Acknowledgment. We thank Professor Helquist for his comments on the rhodium-catalyzed reaction.

References

(1) For recent reviews, leading references, and patents, see (a) Metz, W. A.; Peet, N. P. Inhibitors of Human Neutrophil Elastase as a Potential Treatment for Inflammatory Diseases. *Expert Opin. Ther. Pat.* **1999**, *9*, 851−868. (b) Skiles, J. W.; Jeng, A. Y. Therapeutic Promises of Leukocyte Elastase and Macrophage Metalloelastase Inhibitors for the Treatment of Pulmonary Emphysema. *Expert Opin. Ther. Pat.* **1999**, *9*, 869−895. (c) Leung, D.; Abbenante, G.; Fairlie, D. P. Protease Inhibitors: Current Status and Future Prospects. *J. Med. Chem.* **2000**, *43*, 305−341. (d) Veale, C. A.; Bernstein, P. R.; Bohnert, C. M.; Brown, F. J.; Bryant, C.; Damewood, J. R., Jr.; Earley, R.; Feeney, S. W.; Edwards, P. D.; Gomes, B.; Hulsizer, J. M.; Kosmider, B. J.; Krell, R. D.; Moore, G.; Salcedo, T. W.; Shaw, A.; Silberstein, D. S.; Steelman, G. B.; Stein, M.; Strimpler, A.; Thomas, R. M.; Vacek, E. P.; Williams, J. C.; Wolanin, D. J.; Woolson, S. Orally Active Trifluoromethyl Ketone Inhibitors of Human Leukocyte Elastase. *J. Med. Chem.* **1997**, *40*, 3173−3181. (e) Ohmoto, K.; Yamamoto, T.; Okuma, M.; Horiuchi, T.; Imanishi, H.; Odagaki, Y.; Kawabata, K.; Sekioka, T.; Hirota, Y.; Matsuoka, S.; Nakai, H.; Toda, M.; Cheronis, J. C.; Spruce, L. W.; Gyorkos, A.; Wieczorek, M. Development of Orally Active Nonpeptidic Inhibitors of Human Neutrophil Elastase. *J. Med. Chem.* **2001**, *44*, 1268−1285.

(2) Macdonald, S. J. F.; Belton, D. B.; Buckley, D. M.; Spooner, J. E.; Anson, M. S.; Harrison, L. A.; Mills, K.; Upton, R. J.; Dowle, M. D.; Smith, R. A.; Molloy, C.; Risley, C. Syntheses of *trans*-5-Oxohexahydropyrrolo[3,2-b]pyrroles and *trans*-5-Oxohexahydrofuro[3,2-b]pyrroles (Pyrrolidine *trans*-Lactams and *trans*-Lactones): New Pharmacophores for Elastase Inhibition. *J. Med. Chem.* **1998**, *41*, 3919−3922.

(3) Macdonald, S. J. F.; Dowle, M. D.; Harrison, L. A.; Spooner, J. E.; Shah, P.; Johnson, M. R.; Inglis, G. G. A.; Clarke, G. D. E.; Belton, D. J.; Smith, R. A.; Molloy, C. R.; Dixon, M.; Murkitt, G.; Godward, R. E.; Skarzynski, T.; Singh, O. M. P.; Kumar, K. A.; Hodgson, S. T.; McDonald, E.; Hardy, G. W.; Finch, H.; Fleetwood, G.; Humphreys, D. C. Intracellular Inhibition of Human Neutrophil Elastase by Orally Active Pyrrolidine-*trans*-lactams. *Bioorg. Med. Chem. Lett.* **2001**, *11*, 243−246.

(4) Macdonald, S. J. F.; Dowle, M. D.; Harrison, L. A.; Shah, P.; Johnson, M. R.; Inglis, G. G. A.; Clarke, G. D. E.; Smith, R. A.; Humphreys, D.; Molloy, C. R.; Amour, A.; Dixon, M.; Murkitt, G.; Godward, R. E.; Padfield, T.; Skarzynski, T.; Singh, O. M. P.; Kumar, K. A.; Fleetwood, G.; Hodgson, S. T.; Hardy, G. W.; Finch, H. The Discovery of a Potent, Intracellular, Orally Bioavailable, Long Duration Inhibitor of Human Neutrophil Elastase-GW311616A a Development Candidate. *Bioorg. Med. Chem. Lett.* **2001**, *11*, 895−898.

(5) Macdonald, S. J. F.; Clarke, G. D. E.; Dowle, M. D.; Harrison, L. A.; Hodgson, S. T.; Inglis, G. G. A.; Johnson, M. R.; Shah, P.; Upton, R. J.; Walls, S. B. A Flexible, Practical, and Stereo-

selective Synthesis of Enantiomerically Pure *trans*-5-Oxohexahydropyrrolo[3,2-b]pyrroles (Pyrrolidine-*trans*-lactams), a New Class of Serine Protease Inhibitors, Using Acyliminium Methodology. *J. Org. Chem*. **1999**, *64*, 5166−5175.

(6) In fact, chemical experiments suggested that the acrylamide was a very poor Michael acceptor and the *E*-geometry of the double bond was photostable.

(7) Finke, P. E.; Shah, S. K.; Fletcher, D. S.; Ashe, B. M.; Brause, K. A.; Chandler, G. O.; Dellea, P. S.; Hand, K. M.; Maycock, A. L.; Osinga, D. G.; Underwood, D. J.; Weston, H.; Davies, P.; Doherty, J. B. Orally Active *β*-Lactam Inhibitors of Human Leukocyte Elastase. 3. Stereospecific Synthesis and Structure−Activity Relationships for 3,3-Dialkylazetidin-2-ones. *J. Med. Chem*. **1995**, *38*, 2449−2462.

(8) Frick, L. W.; Adkison, K. K.; Wells-Knecht, K. J.; Woollard, P.; Higton, D. M. Cassette Dosing: Rapid In Vivo Assessment of Pharmacokinetics. *Pharm. Sci. Technol. Today* **1998**, *1*, 12−18.

(9) Such a switch had been observed in an earlier series in the program.

(10) Yoon, N. M.; Kim, E. G.; Son, H. S.; Choi, J. Borohydride Exchange Resin, a New Reducing Agent for Reductive Amination. *Synth. Commun*. **1993**, *23*, 1595−1599.

(11) Application of the reaction mixture to the SCX SPE cartridge was followed by eluting unreacted iodide with EtOH (3 volumes), followed by elution of product with 5% NH_3 in EtOH. Any quaternary ammonium salt is retained on the column. With this process, 24 compounds were purified in 2.5 h.

(12) The amines used were morpholine, methylpiperazine, dicyclohexylamine, piperidine, pyrrolidine, cyclopropylamine, $(^{i}Pr)_2CHNH_2$, dimethylamine, phenylpiperazine, and dibutylamine in 24−93% yields.

(13) The aldehydes used and yields of hydrochlorides were cyclopropylaldehyde (37%), 2,6-dichlorobenzaldehyde (12%), ^{n}PrCHO (37%), PhCHO (68%), and pivalaldehyde (73%).

(14) Videnov, G.; Kaiser, D.; Kempster, C.; Jung, G. Synthesis of Naturally Occurring, Conformationally Restricted Oxazole- and Thiazole-Containing Di- and Tripeptide Mimetics. *Angew. Chem. Int. Ed. Engl.* **1996**, *35*, 1503−1506.

(15) (a) Fujita, E. Organic Synthesis Utilizing Thiazolidine and the Related Heterocycles. *Heterocycles* **1984**, *21*, 41−60. (b) Nagao, Y.; Yamada, S.; Fujita, E. Synthetic Studies on Virginiamycin M2: Functionalization at the 2-Methyl Group of 4-*tert*-Butoxycarbonyl-2-methyl-1,3-oxazole. *Tetrahedron Lett*. **1983**, *24*, 2291−2294.

(16) The amines and yields were piperidine (100%), dimethylamine (100%), pyrrolidine (88%), morpholine (81%), 1-phenylpiperazine (98%), dibutylamine (86%), methylcyclopropylamine (59%), diisopropylamine (36%), and dicyclohexhylamine (26%).

(17) The yields over two steps (hydrolysis and coupling) for the amine derivatives were piperidine (52%), dimethylamine (51%), pyrrolidine (45%), morpholine (93%), 1-phenylpiperazine (47%), dibutylamine (78%), methylcyclopropylamine (21%), diisopropylamine (6%), and dicyclohexhylamine (47%).

(18) A third process for synthesising this oxazole has recently been published by our development chemistry colleagues. Cardwell, K. S.; Hermitage, S. A.; Sjolin, A. A New Method for the Formation of 2,4-Disubstituted Oxazoles: Internal Transfer of Oxidation State Through a Molecular Framework. *Tetrahedron Lett*. **2000**, *41*, 4239−4242.

(19) (a) Connell, R. D.; Tebbe, M.; Gangloff, A. R.; Helquist, P.; Aakermark, B. Rhodium-Catalyzed Heterocycloaddition Route to 1,3-Oxazoles as Building Blocks in Natural Products Synthesis. *Tetrahedron* **1993**, *49*, 5445−5459. (b) Connell, R. D.; Tebbe, M.; Helquist, P.; Aakermark, B. Direct Preparation of 4-Carboethoxy-1,3-oxazoles. *Tetrahedron Lett.* **1991**, *32*, 17−20. (c) Gangloff, A. R.; Aakermark, B.; Helquist, P. Generation and Use of a Zinc Derivative of a Functionalized 1,3-Oxazole. Solution of the Virginiamycin/Madumycin Oxazole Problem. *J. Org. Chem*. **1992**, *57*, 4797−4799.

(20) Clarke, G. D. E.; Dowle, M. D.; Finch, H.; Harrison, L. A.; Inglis, G. G. A.; Johnson, M. R.; Macdonald, S. J. F.; Shah, P.; Smith, R. A. Pyrrolopyrrolone Derivatives as Inhibitors of Neutrophil Elastase, and Their Preparation and Use. PCT Int. Appl. 1999, WO9912933.

(21) Dowle, M. D.; Finch, H.; Harrison, L. A.; Inglis, G. G. A.; Johnson, M. R.; Macdonald, S. J. F. Pyrrolopyrrolone Derivatives as Inhibitors of Neutrophil Elastase. PCT Int. Appl. 1999, WO9912931.

(22) Values were determined by the kinetic methodology described in Weir, M. P.; Bethell, S. S.; Cleasby, A.; Campbell, C. J.; Dennis, R. J.; Dix, C. J.; Finch, H.; Jhoti, H.; Mooney, C. J.; Patel, S.; Tang, C. M.; Ward, M.; Wonacott, A. J.; Wharton, C. W. Novel Natural Product 5,5-*trans*-Lactone Inhibitors of Human α-Thrombin: Mechanism of Action and Structural Studies. *Biochemistry* **1998**, *37*, 6645−6657.

(23) Navia, M. A.; McKeever, B. M.; Springer, J. P.; Lin, T.-Y.; Williams, H. R.; Fluder, E. M.; Dorn, C. P.; Hoogsteen, K. Structure of Human Neutrophil Elastase in Complex with a Peptide Chloromethyl Ketone Inhibitor at 1.84A Resolution. *Proc. Natl. Acad. Sci. U.S.A.* **1989**, *86*, 7−11.

(24) Otwinowski, Z.; Minor, W. Processing of X-ray Diffraction Data Collected in Oscillation Mode. In *Methods in Enzymology*; Carter, C. W., Jr., Sweet, R. M., Eds.; New York: Academic Press, 1997; Vol. 276, pp 307−326.

(25) Navaza, J. AmoRe − an Automated Package for Molecular Replacement. *Acta Crystallogr*. **1994**, *A50*, 157−163.

(26) Murshudov, G. N.; Vagin, A. A.; Dodson, E. J. Refinement of Macromolecular Structures by the Maximum-Likelihood Methodol. *Acta Crystallogr. D* **1997**, *53*, 905−921; CCP4 (Collaborative Computational Project 4).

(27) The CCP4 Suite: Programs for Protein Crystallography. *Acta Crystallogr. D* **1994**, *50*, 760−763.

JM020881F